View metadata, citation and similar papers at core.ac.uk
brought to you by CORE
provided by Repositorio Digital Académico UC Temuco

RESEARCH

Electronic Journal of Energy & Environment
EJE&E
UNIVERSIDAD CATÓLICA DE TEMUCO

Generation and Dispersion Model of Gaseous Emissions from Sanitary Landfills

Alejandro A. Jerez, Luis A. Díaz-Robles and Alberto O. Vergara-Fernández*

Escuela de Ingeniería de Procesos Industriales, Facultad de Ingeniería, Núcleo de Energías Renovables, Universidad Católica de Temuco, Rudecindo Ortega 0259 Campus Norte, Casilla 15-D, Temuco, Chile.

* Corresponding author: Vergara-Fernández A., Telephone: 56-45-205684, Fax: 56-45-205430, E-mail address: avergara@uctemuco.cl.

Received 11 October 2012; revision received 09 February 2013; accepted 09 February 2013. Published online 30 April 2013 (www.ejee.cl). DOI 10.7770/ejee-V1N1-art440.
© Renewable Energies Research Nucleus, UC Temuco.

ABSTRACT A mathematical model was developed to quantify the environmental impact produced by the gases emission from sanitary landfills. The stages of gas generation and diffusion were modeled using waste and cover materials placed in a landfill over an isotropic porous medium, while the dispersion stage was modeled for the atmosphere using a Gaussian model. The United States Environmental Protection Agency (USEPA) criteria were adopted for the estimation of greenhouse gases emissions. The MATLAB computer program was used to prepare simulations of a proposed sanitary landfill to serve the municipalities of Temuco and Padre Las Casas in Chile, considering a lifetime of 20 years. The simulated results show that the conditions of confinement have a greater incidence on the rate of gas emission than does the quantity of waste disposed. It was also concluded that the level of environmental impact varies considerably according to the evaluation scenario and the project design.

KEYWORDS Modeling, landfill, gas emissions, atmospheric pollutants, environmental impact.

Introduction

Environmental impact studies (EIS) of sanitary landfills (SLF) are oriented toward estimating the impact of the construction, operation, and abandonment of these projects generated on the environment, in order to promote reduction or mitigation measures. Although it is important to estimate the transport, visual, economic, and social impact, it is of fundamental importance for the design of control equipment to determine certain effects in the area directly affected, which are associated with the biogas generation (principally CH_4 and CO_2) and leachate [ElFadel et al., 1997]. The biogas generation from organic material can continue for a period of 15 years, and may depending on the aeration conditions in the sector and the waste characteristics, becoming into imminent risks of spontaneous combustion and explosions [ElFadel et al., 1997; Boltze and deFreitas, 1996]. Meanwhile, some studies indicate that biogas emanations may inhibit the growth of plants [Chang et al., 1991; Smith et al., 2005]. A third effect associated with the pollutant emissions into the atmosphere refers to global warming [Gardner et al., 1993; Wanichpongpan

and Gheewala, 2007], and tropospheric ozone formation [Correa et al., 2012].

The Pozo La Feria landfill model considers, for biogas generation, a first order biochemical kinetic and distinguishes between the waste biodegradation behavior with a moderated or a rapid degradation rate [De La Fuente, 1995]. The model of Palos Verdes considers two biodegradation stages with a first order kinetic [EMCOM, 1980]. The model of gaseous emissions from SLF developed by the United States, Environmental Protection Agency (USEPA) is principally oriented toward estimating the emissions of atmospheric pollutants, such as methane, carbon dioxide, and other organic compounds [USEPA, 2005]. The GALIX model proposes two limiting stages for the modeling of the SLF anaerobic system: a fermentation stage and a second methanogenic stage [Behrentz and Giraldo, 1998]. Young and Davies [1992] and Lethlean and Swarbrick [1995] propose simplified kinetic models, emphasizing the thermo-dynamic relationships of the chemical substances present in the SLF, and omitting a greater number of kinetic variables.

Modeling the behavior of the gas in SLFs is usually done on the basis of an isotropic porous medium. Young and Davies [1992] propose the solution of the flow equations in three dimensions for the transitory state, simplifying the geometry of the SLF to the case of a regular solid. Lethlean and Swarbrick [1995] reduce the number of equations, considering a predominantly vertical flow for the migration of the gas within the SLF. Sanchez et al. [2006] carried out extensive computer simulations of gas generation and transport in model landfills under dynamic conditions, using a comprehensive model that they developed. The model was utilized to study the dynamic behavior of landfills, and in particular the pressure distribution and the associated gas concentrations, under a variety of scenarios including cases in which some extraction wells are shut down and/or inserted in the landfill. They showed that the spatial distribution of the permeability has a strong effect on the transient behavior of a landfill and pressure build-up, while mechanical dispersion, manifested by diffusion coefficients that depend on the convective velocities, has virtually no effect on the landfill behavior.

Tchobanoglous et al. [1993] propose two alternatives: a differential model considering the gas generated as a single species, with a predominantly vertical, convection flow. The second model is linear, to estimate the concentration of the components in the gas, with diffusive characteristics.

To model air quality and the dispersion of pollutants, Gaussian models are most widely used, mainly because their equations can be solved easily and because they can provide conservative results [Raufer and Wagner, 1999; USEPA, 1995]. Other authors have include photochemical air quality models, like OZIPR (Ozone Isopleth Package for Research), to asses some Landfill Volatile Organic Compounds (VOCs) on ozone formation in Brazil [Correa et al., 2012], and others have used dispersion modeling approach to asses odorous VOCs released from a main MSW landfill in Istanbul-Turkey [Saral et al., 2009] and North London [Sarkar et al., 2003]. Finally, Figueroa et al. [2009] developed a robust method for estimating landfill methane emissions using MATLAB and an inverse Gaussian air quality model.

The purpose of this study was to quantify the biogas emissions produced by SLF developing a mathematical model, which considers the generation, diffusion, and dispersion of the gases produced by the biodegradation of municipal solid waste (MSW). This study did not include air pollutant reactions around a landfill.

Model Development

Gas production

This model considers the gas generation through a first order kinetic [Spokas et al., 1995], and distinguishes between wastes with a rapid or moderate rate of biodegradation using the Eq. (1) [Gholamifard et al., 2007]:

$$\frac{dG}{dt} = \frac{L_{rb}}{f1} \sum_{i=t+1-(d1+f1)}^{i=t-d1} Bi + \frac{L_{mb}}{f2} \sum_{i=t+1-(d2+f2)}^{i=t-d2} Bi \qquad \text{Eq. (1)}$$

where,

G : Volume of gas produced (m^3).

t : Operating time (s).

L_{mb} and L_{rb}: Potential gas production in MSW of rapid and moderate biodegradation ($m^3 kg^{-1}$).

d_1 and d_2: Biodegradation start time in rapid and moderate biodegradation MSW.

f_1 and f_2 : Period for rapid and moderate biodegradation waste.

B_i : Mass of MSW disposed.

The biodegradable quantity of the MSW is determined from the lignin content, expressed as:

$$B_f = \sum_{i=1}^{n} B_{f,i} X_{pp,i} \qquad \text{Eq. (2)}$$

where,

$B_{f,i}$: Biodegradable proportion of component *i*.

$X_{pp,i}$: Percentage by weight of component *i*.

The cover material required in the design of the daily disposal cell, the accumulated volume of MSW, and average depth of the SLF are calculated according to Tchobanoglous et al. [1993].

Hydric balance and leachate production in SLF

To calculate the leachate generated flow, a hydric balance is realized using the combined levels of MSW disposal, which make up the vertical profile of the SLF. The following equation was used to calculate the water entering the surface cell from the environment [Berger, 2000; Yalçin and Demirer, 2002]:

$$Q_{amb} = K_z A_F \frac{(PP - EVT - ES)}{\Delta z} \qquad \text{Eq. (3)}$$

where,

Q_{amb} : Water flow from the environment into the SLF (m^3 $month^{-1}$).

K_Z : Vertical permeability coefficient (m^2).

A_F : Surface area of the SLF (m^2).

PP : Precipitation on the surface of the SLF (mm $month^{-1}$).

EVT : Water lost through evapotranspiration (mm $month^{-1}$).

ES : Water lost as surface run-off (m^3 $month^{-1}$).

Δz : Thickness of the final cell or covering (m).

The permeability coefficient was determined according to Schroeder et al. [1994]. The surface run-off was estimated using the surface run-off coefficient: $ES = PP - C_{es}$, where C_{es} is the surface run-off coefficient.

The Eq. (4) was used to calculate the flow of lixiviates onto the other cells.

$$Q_{i,j} = Q_{i-1,j} - K_z A_F \left(\frac{Q^{i,j}_{lost,gas} + Q^{i,j}_{stored}}{\Delta z} \right) \qquad \text{Eq. (4)}$$

where,

$Q^{i,j}$: Lixiviates flow in level *i* and month *j* (m^3 $month^{-1}$).

$Q_{lost,gas}{}^{i,j}$: Water flow lost due to gas production in level *i* and month *j* (m^3 $month^{-1}$).

$Q_{stored}{}^{i,j}$: Water flow stored in level *i* and month *j* (m^3 $month^{-1}$).

The volume of water lost due to gas production includes the water consumed in the gas production that is carried off as water vapor contained in the gas. The mass of the MSW contained in the SLF diminishes as it becomes biodegraded, and was calculated using the following equation [Berhentz and Giraldo, 1998; Tchobanoglous et al, 1993]:

$$W'_{MSW} = W_{MSW} - \sum_{j} \Delta G^{i,j} Y_{G/MSW} \qquad \text{Eq. (5)}$$

where,

W'_{MSW} : Mass of MSW remaining after biodegradation in level *i* and month *j* (kg).

W_{MSW} : Mass of MSW in level *i* and month *j* (kg).

$\Delta G^{i,j}$: Gas generation rate in level i and month j (m^3 $month^{-1}$).

$Y_{G/MSW}$: Potential gas production ($kg_{gas}\ kg^{-1}_{waste}$).

The water volume that escapes as saturated vapor was calculated using the ideal gas state equation. The monthly volume of water lost due to gas production was determined by mass balance according to the equation:

$$Q^{i,j}_{lost,gas} = Q^{i,j}_{gas} + Q^{i,j}_{vap} \quad \text{Eq. (6)}$$

where,

$Q_{gas}^{i,j}$: Superficial gas emission from the landfill ($m^3\ s^{-1}$).

$Q_{vap}^{i,j}$: Saturated steam flow with the gas escaped ($m^3\ s^{-1}$).

The water stored in each disposal cell will define the quantity of water, which will effectively percolate to underground levels. For each disposal level there is a water storage capacity threshold, established by the field capacity, the degree of drying, and the humidity content of the MSW. This capacity can be expressed through the Eq. (7):

$$Q^{i,j}_{stored} = Q^{i,j}_{fc} - Q_{DD} - Q^{i,j}_{Hum} \quad \text{Eq. (7)}$$

where,

$Q_{fc}^{i,j}$: Saturated steam flow with the gas escaped ($m^3\ month^{-1}$).

Q_{DD} : Water present only in the final covering, depending on the degree of drying, in level i and month j ($m^3\ month^{-1}$).

$Q_{Hum}^{i,j}$: Water in the disposal cell in level i and month j ($m^3\ month^{-1}$).

The field capacity is a function of the weight of added load above the mean level of the MSW in each of the disposal cells [Behrentz and Giraldo, 1998; Tchobanoglous et al., 1993]. The weight of added load for each cell was estimated according to Tchobanoglous et al. [1993]. The density of the MSW in the SLF increases with the depth of the disposal level. Settling of the SLF will occur, due to the loss of mass in the form of gaseous components and leachate during the biodegradation process; to the added load produced by the addition of disposal levels; and to the entrance and exit of water through the SLF.

Generation of meteorological data

The variables considered in the generation of meteorological data are precipitation, temperature, solar radiation, wind speed, and atmospheric humidity. Normal distribution functions were used to generate these meteorological data: Gamma, Weibull and Uniform [Schroeder et al., 1994; Semenov and Barrow, 2002]. A time series of simulated data for real evapotranspiration was generated using Turc's empirical model [Vadillo and Carrasco, 2005], accumulated monthly precipitation and mean monthly temperature.

Wind information was based on data from historical records of monthly frequency of observation for the predominant wind direction and mean speed over the area of influence.

Estimates were made of the combined frequency of observation of wind speed, cloud cover, and sunshine and the combined frequency of atmospheric stability category and predominant wind direction were estimated.

Model for gas flow inside the SLF

The vertical transport by convection through the disposal levels of MSW of the gas generated, taking into account the average depth of the SLF adjusted for settlement, was evaluated using the Eq. (8) proposed by Young and Davies [1992]:

$$\frac{\partial p}{\partial t}\frac{\varphi+\gamma\theta}{P_{atm}} = K_z\frac{\partial^2 p}{\partial z^2} + \frac{G}{\rho};\ \frac{1}{\rho} = \frac{RT}{PM\ P_{atm}} \quad \text{Eq. (8)}$$

where,

p : Pressure (atm).

φ *and* θ : Porosity of the SLF when saturated with

gas and water.

γ : Henry's constant.

P_{atm} : Atmospheric pressure (atm).

z : Spatial co-ordinate of the locations of the facility and receptor in the study area (m).

ρ : Gas density (kg m^{-3}).

R : Ideal gas constant: 8.2057x10^{-5} (atm m^3 mol^{-1} $^oK^{-1}$).

T : Gas temperature (^{o}C).

PM : Molecular weight of the gas (kg $kgmol^{-1}$).

For the sake of convenience, each disposal level of the MSW was considered as a finite element. The expression $G_{i/\rho}$ varies for each disposal level according to the age and depth of the disposal. It is assumed that the pressure is in equilibrium with atmospheric pressure prior to the generation of gas in the SLF [Gebert and Groengroeft, 2006]. The initial and border conditions are taken as follow:

$$\text{I.C. } P_{i,1}\Big|_{t=0} = P_{atm} \qquad \text{Eq. (9)}$$

$$\text{B.C.1 } P_{1,j+1}\Big|_{z=0} = P_{atm} \ (i=1 \text{ for surface } z=0) \qquad \text{Eq. (10)}$$

$$\text{B.C.2 } \frac{P_{n+1,j+1} - P_{n,j+1}}{\Delta z}\Bigg|_{Z=Z\max} = 0 \qquad \text{Eq. (11)}$$

(base of the landfill $z=z_{max}$)

where,

P_{atm} : Atmospheric pressure (atm).

P : Pressure (atm).

z : Spatial coordinate of the locations of the facility and receptor in the study area (m).

Emissions of gases at the surface of the SLF

Whether the pore size in the cover soil layer is in average relatively high, such as when the cover material is permeable or there is low compaction, the adjustment to the equilibrium "air-landfill" will be achieved quickly. On the other hand, soil covers with small average pore size will tend to respond slower compared to changes in atmospheric pressure [Gebert and Groengroeft, 2006]. For this case, the Darcy's law is proposed to evaluate the flux density gas emission from the landfill surface described by the Eq. (12) and discussed in the studies of Young and Davies [1992] and Yen-Cho et al. [2003].

$$F_{gas} = K_z\left(\frac{\overline{p} - P_{atm}}{\Delta z}\right) \qquad \text{Eq. (12)}$$

where,

F_{gas} : Volumetric flux density emission of the gas (m3 m-2 s-1).

$\overline{p}$: Average value of absolute static pressure (atm).

P_{atm} : Atmospheric pressure (atm).

Δz : Thickness of surface coverage of the landfill (m).

Kz : Vertical permeability of the surface or final landfill cover.

Emission of gases from passive extraction systems

The pressure at any distance from the extraction well depends on the absolute static pressure and on its disturbance by the extraction well [Yen-Cho et al., 2003]. The absolute static pressure is approximately constant across the whole radial distance whether homogeneity is maintained over the whole surface of the SLF. For the effects of quantification, the radius of influence is defined as the radial distance to extraction well for which the difference between the absolute static pressure and the absolute extraction pressure is zero

[Gebert and Groengroeft, 2006]. The total pressure of the SLF is given by [Young and Davies, 1992]:

$$p = p_0 + \sum_{i=1}^{n} V_i \cdot F_i \; ; V_i = \beta_i \left(p_i - \sum_{j \neq 1}^{n} \mu_{i,j} p_j \right) + \alpha_i \qquad \text{Eq. (13)}$$

where,

p_0 : Absolute static pressure without extraction wells (atm).

V_i : Gas flow extracted by the well i'esima ($m^3 s^{-1}$).

F_i : Relationship between volumetric gas flow extracted and the pressure in the well i'ésima (atm s m^{-3}).

β_i : Empirical coefficient.

$\mu_{i,j}$: Coefficient of yield reduction for extraction well i as a function of the pressure in extraction well j.

p_i : Internal pressure of extraction in the well i'esima (atm).

p_j : Internal pressure of extraction in la well j'esima (atm).

α_i : Empirical coefficient.

The internal extraction pressure in the wells was calculated as a flow pressure:

$$p_{\text{int}} = \overline{p} - p_{flue.} \qquad \text{Eq. (14)}$$

where,

p_{int} : Internal pressure exhaust in any well (atm).

p_{flue} : Absolute internal pressure in any well (atm).

$\overline{p}$: Average value of absolute static pressure (atm).

The performance reduction coefficient is exponentially related to the distance between wells:

$$\mu_{i,j} = k_1 \cdot e^{-k_2 \cdot d_{i,j}} \qquad \text{Eq. (15)}$$

where,

k_1 and k_2: Empirical adjustment coefficients.

$d_{i,j}$: Distance between wells i and j (m).

Dispersion of gases emitted by the SLF

The following expression was used to obtain the maximum altitude, which the displaced air mass may reach [Raufer and Wagner, 1999]:

$$z_{\text{max,i}} = z_{\text{F,i}} + \frac{v_{\text{F,i}}}{\sqrt{\left(\frac{\partial \theta}{\partial z}\right)_i \cdot \frac{g}{T_i}}} \qquad \text{Eq. (16)}$$

where,

$z_{max,i}$: Maximum altitude attainable by an airmass which is initially displaced to the altitude of the preferential flow surface *i* (masl).

$z_{F,i}$: Altitude of the preferential flow surface *i* (masl).

$v_{F,i}$: Velocity of the air mass at the preferential flow surface (m s^{-1}).

$(\partial\theta/\partial z)_i$: Vertical gradient of potential temperature at altitude *i* (°C m^{-1}).

g : Gravitational constant (m s^{-2}).

T_i : Atmospheric temperature at altitude "*i*" (°C).

A wind field was configured on a grid based on preferential flow surfaces. The interaction between the lower atmosphere and the ground surface follows the movement conservation equation, generating a speed profile in the limit layer. Consequently, for the interpolation of the horizontal components of the wind vector in the columns of grid, the law of powers is used [Irwin et al., 2000]. All points of the new grid are identified by a pair of geographical coordinates and by an altitude value for the preferential flow surface. The values of the wind speed vector components are adjusted in order to obtain a field with zero diver-

gence according to the hypothesis of incompressible fluids.

Finally, atmospheric turbulence was described in a grid in which each point is a vector with three components. Given that atmospheric flow tends to follow the curves of the ground surface, the vertical component of the wind speed vector was obtained by the following equation:

$$w = \bar{v} \cdot \nabla H \qquad \text{Eq. (17)}$$

where,

w : Vertical component of the wind speed vector.

$\bar{v}$: Component of the wind speed vector.

∇H : Ground curve vector (gradient).

Gaussian model of gas dispersion in the atmosphere

The Gaussian solution for the mass transport equation under an atmospheric turbulent flow is [Raufer and Wagner, 1999]:

$$C_i = \frac{S_i \cdot \left(e^{\left(\frac{-y^2}{(2\cdot\sigma_y^2)} + \frac{-(z-H)^2}{(2\cdot\sigma_z^2)} \right)} + e^{\left(\frac{-y^2}{(2\cdot\sigma_y^2)} + \frac{-(z+H)^2}{(2\cdot\sigma_z^2)} \right)} \right)}{(2 \cdot \pi \cdot \sigma_y \cdot \sigma_z \cdot \bar{u})} \qquad \text{Eq. (18)}$$

where,

C_i : Concentration of pollutants in receptor (mg m^{-3}).

S_i : Rate of pollutant emission (kg s^{-1}).

z, x and y : Spatial coordinates of the locations of the facility and receptors in the study area (m).

σ^2_y and σ^2_z : Dispersion coefficients in directions x, y and z (m^2). These depend on the atmospheric stability.

$\bar{u}$: Mean wind speed (m s^{-1}) at 10 m high.

H : Altitude of emission of pollutants (m).

The Gaussian plume shows that the concentration over the plume of a pollutant continuously emitted is proportional to the emission rate, and in addition, it is diluted by the wind speed on the emission point at a rate inversely proportional to the wind speed [Irwin et al., 2000].

The Gaussian model for are sources requires the integration of all points that conform the surface emission. The integration of the Gaussian solution becomes undetermined for all the receptors that are close of the emission surface. To avoid this error, the emission surface is calculated as a finite emissions summation of punctual type, considering a set of 400 points generated as gridded cells over the landfill.

The joint frequencies due to a division of the entire area around the emission source in at least 16 sectors correspond to 16 possible wind directions. The wind speed is divided in 6 increasing order categories. The frequency of joint occurrence is evaluated over a long period of time and for each sector, for each wind speed category, and for each category of atmospheric stability. It generates a total of at least 576 values of joint frequency [Irwin et al., 2000]. The weighted value of wind speed for each predominant wind direction is:

$$VV_\theta = \sum_{i=vv}^{6} CV_{\theta,vv} \cdot f_{\theta,vv} \qquad \text{Eq. (19)}$$

where,

VV_θ : Annual weighted wind speed for the θ^{th} predominant wind direction (m s^{-1}).

$CV_{\theta,vv}$: Central value of the vv^{th} wind speed category in the θ^{th} predominant wind direction (m s^{-1}).

$f_{\theta,vv}$: Frequency of the annual average observation from the historic records of the influence area for the vvth wind speed category in the θ^{th} predominant wind direction.

In the case of the atmospheric stability category for each predominant wind direction, the weighted value corresponds to the modal value. The Gaussian

Table 1 Entry values of the physical properties of the MSW for the simulation.

Variable	Value	Units	Reference
Disposal rate of MSW	223	Ton d^{-1}	---
Density of MSW	220	kg m^{-3}	CEPIS [1998]
Porosity of MSW	0.67	m^3 m^{-3}	Schroeder et al. [1994]
Humidity content of MSW	0.18	m^3 m^{-3}	CEPIS [1998]
Intrinsic vertical permeability of MSW	1.6×10^{-12}	m^2	Schroeder et al. [1994]

Table 2 Comparison of projected population growth for the municipalities of Temuco and Padre Las Casas, using geometric, vegetative and exponential methods.

Projected population	Geometric	Vegetative	Exponential
Total (inhab.)	308,750	302,020	309,630
Error against 2002 census	2.42 %	0.19 %	2.72 %

plume model of long-term for gaseous pollutants released from the landfill surface is described by the Eq. (20):

$$C_i(x,y,z) = \sum_{\theta=\theta_1}^{\theta_{16}} f_\theta \cdot \sum_{p=1}^{400} \frac{Q_{gas}}{400} \cdot \left(\frac{e^{\left(\frac{-y^2}{(2\cdot\sigma_{y,\theta}^2)}+\frac{-(z-H)^2}{(2\cdot\sigma_{z,\theta}^2)}\right)} + e^{\left(\frac{-y^2}{(2\cdot\sigma_{y,\theta}^2)}+\frac{-(z+H)^2}{(2\cdot\sigma_{z,\theta}^2)}\right)}}{(2\cdot\pi\cdot\sigma_{y,\theta}\cdot\sigma_{z,\theta}\cdot\bar{u}_{,\theta})} \right)$$

Eq. (20)

where,

f_θ : Frequency of observations for the θth predominant wind direction.

Q_{gas} : Gas flow (m^3 s^{-1}).

Results and discussion

A simulation was made of an SLF project for the MSW disposal of the Temuco and Padre Las Casas municipalities, Araucanía Region, Chile. The location and area of influence of the project was defined arbitrarily within the municipal area of Temuco, however, it was considered that the city of Temuco was designed as non-attainment area for PM_{10} (the fraction of particulates in air with an aerodynamic diameter ≤ 10 μm) air pollution in 2005 [Díaz-Robles et al., 2008]. Information on the description of the project and the base line of the area of influence was obtained from the following sources:

- Environmental Impact Study, Improvement Project, Centre for the Final Disposal of Municipal Solid Waste, Municipality of Temuco. National Environmental Commission (CONAMA) – Chile.
- 25 Years of Agrometeorological Observations. Agrometeorological Station Carillanca - Chile.
- Regional Statistical Synthesis 2001 IX Region, Chile.
- Preliminary Results – Census 2002-Chile.

Table 1 shows the entry values of the physical properties of the MSW required for the simulation. The total population was estimated from historical records. The variation between the 1992 and the 2002 census for the combined population of the municipalities of Temuco and Padre Las Casas is 23.76% and the overestimate is at least 2.78%. With an annual growth rate of 2.4% and taking 1992 as the base year, the population for the two municipalities was projected using the three methods selected, as shown in Table 2.

The values used to estimate the variation in the rate of MSW disposal during and operating period

Table 3 Entry values for estimating the variation in the rate of MSW disposal.

Variable	Value
Opening year	2003
Opening month	March
Year of closure	2023
Month of closure	October
Population served in start year	302,020 inhab.
Annual population growth rate	2.4%
Rate of MSW generation	0.738 kg inhab^{-1} d^{-1}
Annual variation in the rate of MSW generation (CEPIS, 1998)	2%
Projection of population growth	Vegetative

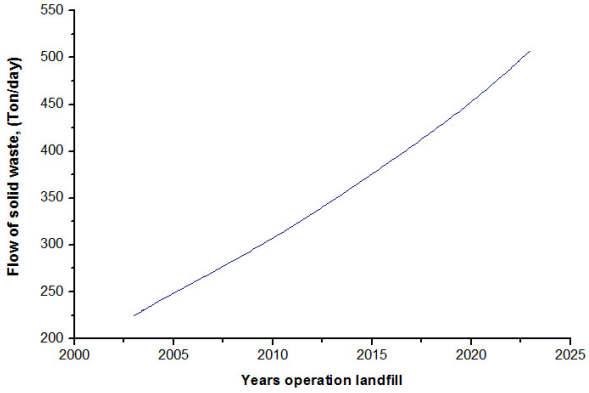

Figure 1 Annual variation in the daily disposal rate of MSW in the municipalities of Temuco and Padre las Casas (Chile) for the useful life of the Sanitary Landfill.

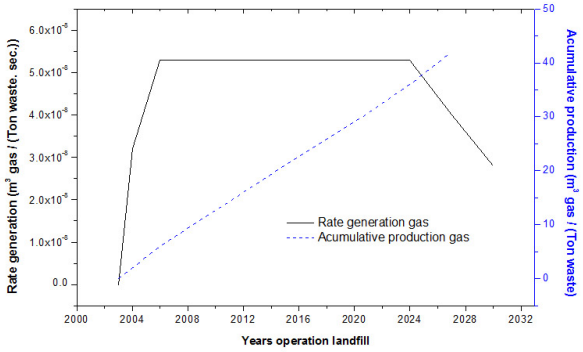

Figure 2 Rate of gas generation and cumulative gas production per ton of waste. La Feria's model.

of 20 years are summarized in Table 3. The estimated annual variation for the daily rate of MSW disposal is shown in Fig.1.

A total area of 12.73 hectares was taken for the study. The information for laying out the MSW disposal area is elevation, Latitude (UTM), Longitude (UTM), Altitude (masl), Gradient (%/100). The area of influence lies within the coordinates 5710000 - 5720000 latitude south, and 700000 - 710000 longitude west. All the topographical information on the site for the area of influence was entered using contour lines.

To generate the meteorological information, the accumulated monthly historical data for the period between 1964 and 1988 were entered. These were data recorded by the Carillanca Experimental Station (38°41´40.10"S, 72°25´02.16"O, Elev. 190 m), Temuco, Chile.

To estimate gas generation, a simulation was made of the MSW disposed of in the SLF, using La Feria's model (Table 4 shows the data for the simulation of the model). The variation in time of the rate of generation and cumulative production of gas per ton of waste is shown in Fig. 2. The calculations show that the potential value for the volume of gas produced from MSW with rapid biodegradation is 16% greater than for that produced from MSW with moderate biodegradation. With regard to gas generation rates, La Feria's model gives a constant maximum value of 0.005 L kg^{-1} d^{-1}.

In order to compare the variation over time of the

Table 4 Entry values in the La Feria gas generation model

Variable	Value	Units	Reference
Rapid biodegradation waste			
Total fermentation period	24	month	De La Fuente [1996]
Period to start of biodegradation	2	month	De La Fuente [1996]
Biodegradable fraction by weight	0.107	kg kg^{-1}_{MSW}	---
Potential gas production	0.155	m^3 kg^{-1}_{MSW}	---
Moderate biodegradation waste			
Total fermentation period	120	month	De La Fuente [1996]
Period to start of biodegradation	8	month	De La Fuente [1996]
Biodegradable fraction by weight	0.041	kg kg^{-1}_{MSW}	---
Potential gas production	0.133	m^3 kg^{-1}_{MSW}	---

Table 5 Dimensions of the sanitary landfill and comparison of the simulated results for the three scenarios.

Variable	Scenario 1	Scenario 2	Scenario 3	Units
Area covered by waste	7	12.726	12.726	hectares
Settling depth	23.82	62.19	66.5	m
Density of emission flow	3.17×10^{-5}	1.5×10^{-5}	2.2×10^{-11}	m^3 m^{-2} s^{-1}
Total surface emission	350000	927000	0.25	m^3 d^{-1}

behavior of the SLF as a source of gas emissions, three simulated scenarios were prepared for the years 2008, 2022 and 2028. Table 5 summarizes the dimensions of the SLF for the three simulated scenarios. Figs. (3) and (4) show the adjustment of the vertical profile of the SLF for the third scenario, taking account of settling caused by the pressure of added load, the leachate content per level of disposal, and the loss of MSW mass due to biodegradation.

In the first simulated scenario, there is a significant increase in the density of the MSW, from 960 to 1050 kg m^{-3}, as the depth increases. This situation stabilizes from a depth of 5 m, due to the age of biodegradation of the MSW. The deepest level of the SLF presents a density of 1035 kg m^{-3}. As a result of these four simultaneous processes, the average depth of the SLF initially estimated for the first scenario varies from 32 m to a corrected depth of 24 m. According to Tchobanoglous et al. [1993] a variation of up to 40% in the depth of the disposed matter can be expected, due to settling of the SLF. Based on these calculation criteria, the average depth of MSW varies from 82 to 61 m for the second simulated scenario, and from 86 to 66 m for the third scenario. The values reported range from 10 m [Walter, 2002] and 26 m [Department of the Army USA, 1995], to 120 m [Tchobanoglous et al., 1993].

Table 5 summarizes the flow of gases emitted from the surface, calculated for the three simulated scenarios. Fig. 5 presents a diagram of the diffusion of the gas through the vertical profile of the SLF for the third simulated scenario.

To calculate the rate of gas emission from the SLF through the diffusion model, an estimate was made of the conditions of confinement of the MSW expected in the project and the interaction between the SLF

Table 6 Entry values for the two passive extraction system designs.

Variable	Value	Units	Reference
Pressure in extraction well	1	atm	Walter [2002]
Co-efficient alpha	26	$m^3\ h^{-1}$	Young et al. [1992]
Co-efficient beta	0.028	$m^3\ Pa^{-1}h^{-1}$	Young et al. [1992]
Constant k1	0.0215	-	Young et al. [1992]
Constant k2	0.1362	m^{-1}	Young et al. [1992]
Surface oxidation of methane	20	%	---
Efficiency of combustion in well	95	%	---

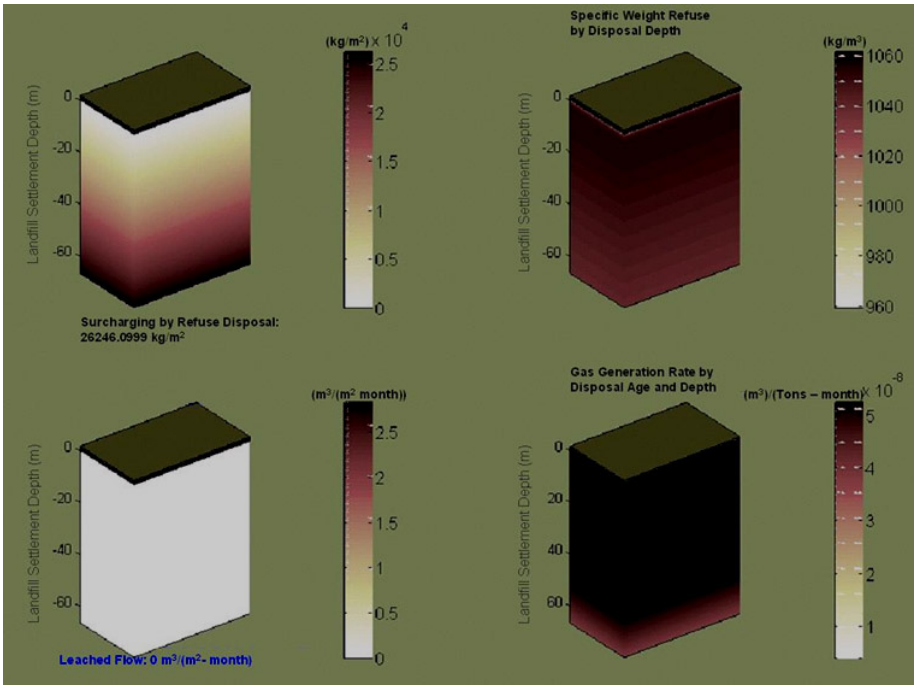

Figure 3 Disposal of MSW and dynamic behavior of the Sanitary Landfill. Scenario 3.

and the external medium. The first step was to determine the dimensions of the SLF and their variation over time. For a period of twenty years, the rate of MSW disposal is expected to double towards the end of its useful life, from 223 tons today to over 500 tons (see Fig. 1). This result is based on the population growth of the two municipalities and the sustained increase in the rate of refuse generation per capita (2% per year proposed by CEPIS [1998]).

For the first scenario, the model predicts a maximum deviation in atmospheric pressure of 9% (9.12 kpa of relative pressure). For the other two simulated scenarios, the absolute static pressure does not fluctuate by more than 3%. Consequently, the volumetric flow density of gas migration into the atmosphere from inside the SLF is slightly greater in the first scenario than in the second, $3.17x10^{-5}$ and $1.5x110^{-5}$ $m^3\ m^{-2}\ s^{-1}$, respectively.

For each simulated scenario, two designs are considered for the passive extraction system: design 1 with wells every 35 m and design 2 with wells every 55 m. The values used for these designs are shown in Table 6. The result of the gas flow per extraction well for the third scenario is presented in Fig. 6.

In the first design (wells placed every 35 m), according to the planned area for the reception of MSW, 29 wells were calculated for the evacuation of gas from the 7 hectares covered in the first simulated scenario. The extraction flow per well varied from 0.03 to 0.05 $m^3 s^{-1}$. With a distance of 55 m between wells, for the same scenario, the number of wells is reduced to 10. In this case the variation of the gas flow per well is only between 0.068 and 0.070 $m^3 s^{-1}$, given that the interaction effect in the migration of the static flow of gas within the SLF is reduced. Although the extraction flow per well is greater for the second design, when the estimates of the total gas flow through all the wells are compared the first design presents greater efficiency in the evacuation of gas into the atmosphere, with 86000 $m^3 d^{-1}$ as opposed to 57500 $m^3 d^{-1}$. Similar behavior to the first simulated scenario was estimated for the second and third scenarios. For the-

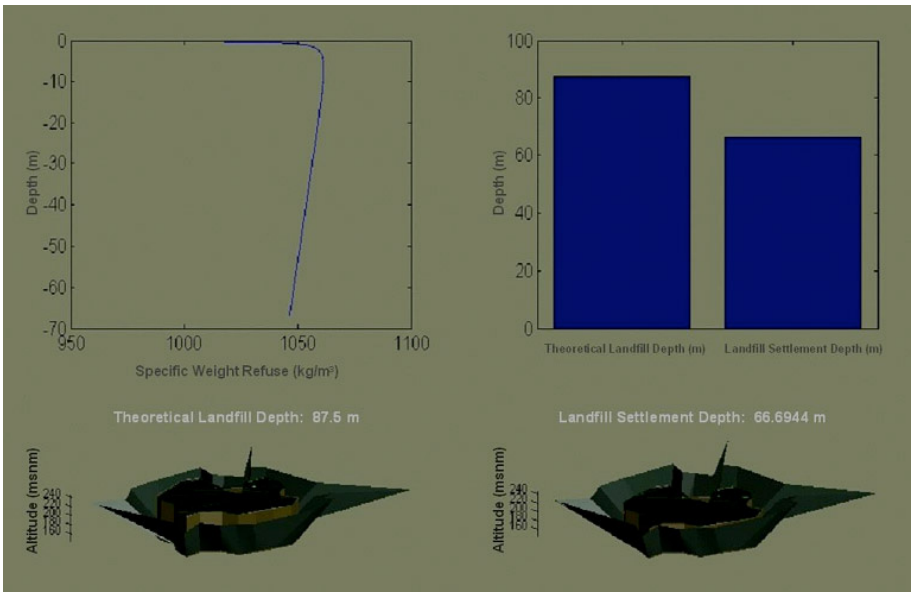

Figure 4 Settling calculation for the Sanitary Landfill. Scenario 3.

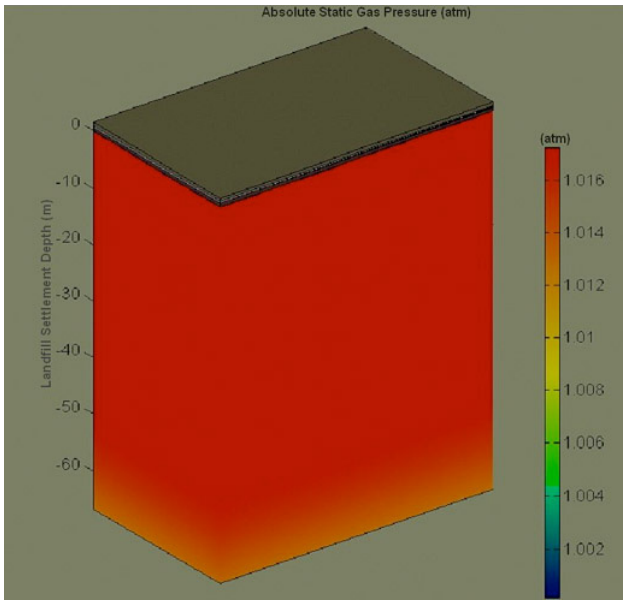

Figure 5 Gas diffusion inside the Sanitary Landfill for the third simulated scenario.

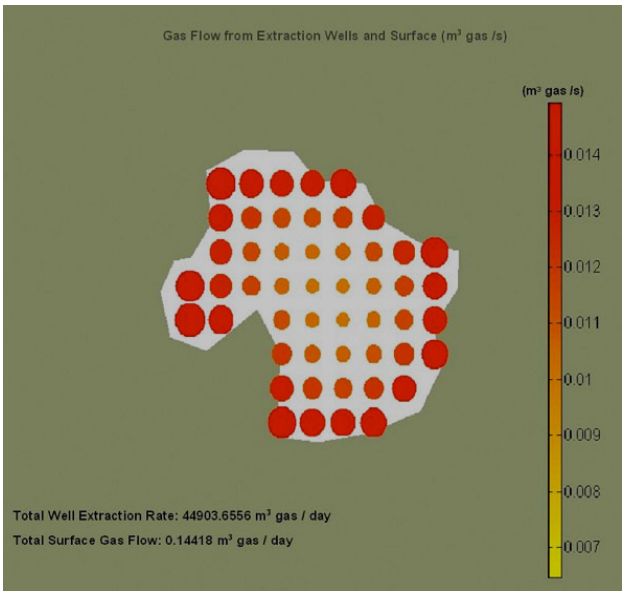

Figure 6 Gas emissions from the surface and through the passive extraction system for design 1 of the third simulated scenario.

Table 7 Simulated results for the three scenarios and the two designs (passive extraction system). Maximum gas concentration – inmision height.

Variable	Scenario 1		Scenario 2		Scenario 3		Units
	Design 1	Design 2	Design 1	Design 2	Design 1	Design 2	
Maximum gas concentration	57.35	54.79	21.14	20.92	2.79	1.89	ppm vol.

se scenarios the disposal area has been completed, causing the number of wells to increase to 51, when placed 35 m apart, and 20, when placed 55 m apart. In the case of the first design, there is a greater variation between the gas flow evacuated from the wells nearest the perimeter and those in the centre in the third scenario than in the second. In the third scenario the flow per well varies between 0.008 and 0.02 $m^3\ s^{-1}$, while in the second it varies between 0.009 and 0.016 $m^3\ s^{-1}$. For a distance of 55 m, the estimated gas flow per well is slightly greater for the third scenario, where it varies between 0.0255 and 0.0265 $m^3\ s^{-1}$, than the second, where the variation is between 0.0195 and 0.0205 $m^3\ s^{-1}$. In both cases, the gas flows per well are lower than the results estimated for the first scenario.

The combination of the final covering and the extraction wells means that the total gas flow from inside the SLF five years after its closure (third simulated scenario) will for practical purposes be exclusively through the extraction wells. The gas flow by surface emission was only 0.25 $m^3\ d^{-1}$, insignificant when compared to the 41300 $m^3\ d^{-1}$ expected for the second design. On the other hand, while the SLF is still in operation under the second scenario, the gas flow through surface emission (fugitive or non-controlled emission) may reach up to 30 times the expected flow of 32000 $m^3\ d^{-1}$ for design 2.

The simulated values for the gas flow per well are within the range of results of the simulations made by Young and Davies [1992] and Sanchez et al. [2006]. They are also not dissimilar to the values reported from field studies by Walter [2002], between 0.0046 and 0.24 $m^3\ s^{-1}$ for active collection systems.

Table 7 shows a comparison of the maximum gas concentration expected for all the combinations of simulated scenarios and extraction system designs on a yearly basis, considering weighting for the wind. Fig. 7 shows a spatial profile of maximum emission height of the gas concentration emitted from the SLF for the third simulated scenario and design 1 of the passive extraction system.

The plume dispersion in the surroundings of the

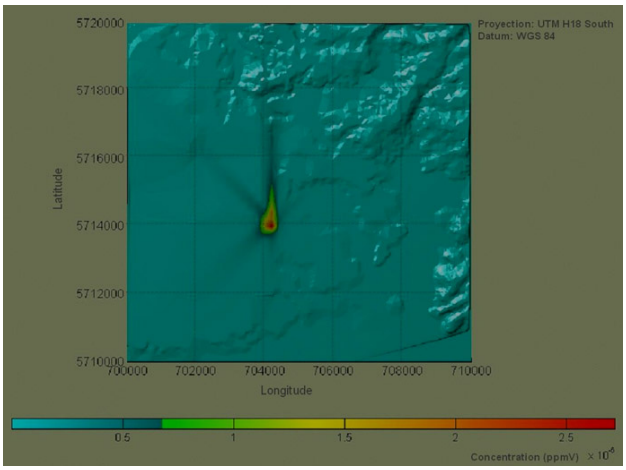

Figure 7 Annual weighting for pollutant dispersion in the area of influence. Design 1 - Scenario.

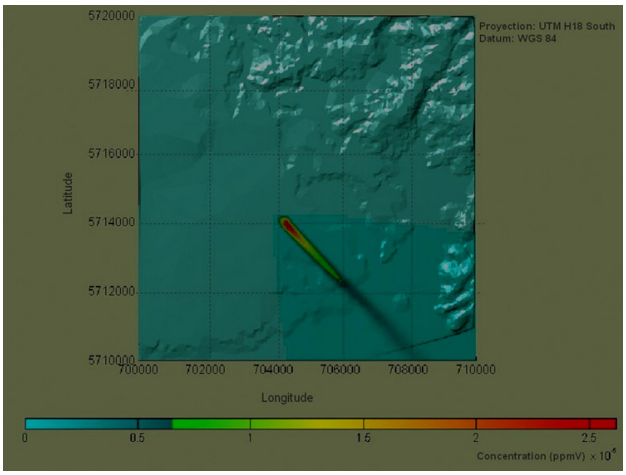

Figure 8 Pollutant dispersion. Slightly stable atmosphere. Design 1 - Scenario 1.

Table 8 Episode of specific meteorological conditions.

Variable	Episode	Units
Atmospheric stability	Slightly stable	-
Atmospheric pressure(1)	1	atm
Air temperature (1)	25	ºC
Relative air humidity (1)	65.4	%
Wind velocity(1)	2.8	m s^{-1}
Predominant wind direction (1)	Southeast	-
Vertical temperature gradient	0.015	ºC m^{-1}
Maximum altitude of estimate	500	masl
(1): Using meteorological data at the inmision height (1.5 m from ground level).		

landfill could be determined from the average emission rate, the topography and the local meteorological data at the considered time. Table 8 summarizes the specific meteorological conditions which determine wind patterns on an hourly scale for each episode simulated. Fig. 8 shows a spatial profile maximum emission height of the gas concentration emitted from the SLF, under the wind patterns on an hourly scale. The values for the maximum gas concentration in the environment oscillate between 1.9 and 57.3 ppm of atmospheric air. These areas of maximum concentration coincided with important places from the standpoint of public health. Policy-makers should take into account these aspects along with economic considerations if protection of the public health is one of their major concerns.

Conclusions

The modeling and simulation techniques are an appropriate prediction tool for the evaluation of the environmental impact of SLF projects. The heterogeneous conditions affecting the transport of materials in the SLF make it difficult to estimate diffusion models.

The results of the simulation predict that the conditions of confinement in the SLF will be of greater importance for the gas emission process than the quantity of MSW disposed of. They likewise predict the importance of the design of the final covering of the landfill for the quantity of gas emitted, and therefore for the estimated levels of air pollution.

The tendency of the pollutants to disperse, seen in the stationary plume under the weighted wind conditions for the area of influence, is towards the predominant directions of the north and northeast. The maximum gas concentration values estimated for the immediate surroundings of the SLF are significantly lower for the third scenario, due to the existence of the final covering and the consequent mitigation of surface emissions from the SLF. Meanwhile, as regards the concentration of gas in the medium, the results generated in the simulation indicate that the design of the passive collection system does not have a major incidence, with estimated values for designs one and two being practically the same.

References

Behrentz, E. and Giraldo, E. (1998). Coupled model for estimation of gas generation and leachate production (GALIX). In: Fifth Latino-American Workshop and Seminar of Wastewater Anaerobic Treatment. Viña del Mar, Chile.

Berger, K., (2000). Validation of the hydrologic evaluation of landfill performance (HELP) model for simulating the water balance of cover Systems. Environmental Geology. vol. 39, nº 11, 1261 – 1274. DOI: 10.1007/s002549900090.

Boltze, U., deFreitas, M.H., (1996). Changes in atmospheric pressure associated with dangerous emissions from gas generating sites. The 'explosion risk threshold' concept. Proceedings of the Institution of Civil Engineers-Geotechnical Engineering. vol. 119, nº 3, 177-181. DOI: 10.1680/igeng.1996.28509.

Chang, G.Y.S., Wong, M.H. and Whitton, B.A., (1991). Effects of landfill gas on subtropical woody-plants. Environmental Management. vol. 15, nº 3, 411-431. DOI: 10.1007/BF02393888.

Centro Panamericano de Ingeniería Sanitaria y Ciencias del Ambiente – Organización Panamericana de la Salud, CEPIS – OPS, Marzo (1998). Análisis Sectorial de los Residuos Sólidos en Chile. http://www.cepis.ops-oms.org/

Corréa, S.M., de Souza, C.V., Sodré, E.D., and Teixeira, J.R. (2012). Volatile Organic Compound Emissions from a Landfill, Plume Dispersion and the Tropospheric Ozone Modeling. J. Braz. Chem. Soc., Vol. 23, nº 3, 496-504.

De La Fuente, M.L., Estudio de la producción de biogás en una unidad experimental de un relleno sanitario, Santiago. (1995), Universidad de Chile: Santiago.

Department of The Army U.S.A, April (1995). Engineering and design landfill off-gas collection and treatment systems. U.S.A Army Corps Of Engineers Cemp-Rt, Washington.

Díaz-Robles, L.A., Ortega-Bravo, J.C., Fu, J.S., Reed, G.D., Chow, J.C., Watson, J.G. and Moncada, J.A. (2008). A Hybrid ARIMA and Artificial Neural Networks Model to Forecast Particulate Matter in Urban Areas: The Case of Temuco, Chile. Atmospheric Environment. Vol. 42, nº 35, 8331-8340.

ElFadel, M., Findikakis, A.N. and Leckie, J.O., (1997). Environmental impacts of solid waste landfilling. Journal of Environmental Management. Vol. 50, nº 1, 1-25. dx.doi.org/10.1006/jema.1995.0131.

EMCOM Associates, (1980), Methane generation and recovery from landfill. Ann. Arbor Sc. Publishers. Ann Arbor, MI.

Figueroa V.K., Mackie K.R., Guarriello, N., and Cooper, C.D. (2009). A Robust Method for Estimating Landfill Methane Emissions. Journal of the Air & Waste Management Association. Vol. 59, nº 8, 925–935.

Gardner, N., Manley, B.J.W. and Pearson, J.M., (1993). Gas emissions from landfills and their contributions to global warming. Applied Energy. vol. 44, nº 2, 165-174. dx.doi.org/10.1016/0306-2619(93)90059-X.

Gebert, J. and Groengroeft, A., (2006). Passive landfill gas emission – influence of atmospheric pressure and implications for the operation of methane-oxidising biofilters. Waste Management. vol. 26, nº 3, 245–251. dx.doi.org/10.1016/j.wasman.2005.01.022

Gholamifard, S., Duquennoi, C. and Eymard, R., (2007). A multiphase model of bioreactor Landfill With Heat And Gas Generation And Transfer. in Eurotherm Seminar n° 81, Reactive Heat Transfer in Porous Media. Ecole des Mines d'Albi, France.

Irwin, J.S., Chico, T., Catalano, J., Turner, D.B., (2000). CDM 2.0 - Climatological dispersion model user's guide. Meteorology and assessment division, atmospheric sciences research laboratory, Office of Research and Development, U. S. Environmental Protection Agency and Aerocomp, Inc.

Lethlean, J.J. and Swarbrick, G.E., (1995). The use of thermodynamics to model the biodegradation processes in municipal solid waste landfills. MODSIM 95: International Congress on Modelling and Simulation, vol. 1, 238-242.

Sanchez, R., Hashemi, M., Tsotsis, T.T., and Sahimi, M., (2006). Computer simulation of gas generation and transport in landfills II: Dynamic conditions. Chemical Engineering Science. Vol. 61, nº 14, 4750–4761

Saral, A., Demira S., Yıldız, S. (2009). Assessment of odorous VOCs released from a main MSWlandfill site in Istanbul-Turkey via a modelling approach. Journal of Hazardous Materials. Vol. 168, 338–345.

Sarkar, U., Hobbs, S.E., and Longhurst P. (2003). Dispersion of odour: a case study with a municipal solid waste landfill site in North London, United Kingdom. Journal of Environmental Management. Vol. 68, nº 2, 153–160.

Schroeder, P., Lloyd, C., Zappi, P. and Aziz, N., (1994). Hydrologic evaluation of landfill performance (HELP) model: User's Guide for Version 3, EPA/600/R-94/168b. United States, Environmental Protection Agency: Washington, D.C.

Semenov, M.A. and Barrow, E.M., (2002). LARS-WG: A stochastic weather generator for use in climate impact studies, Version 3.0, User Manual. Rothamsted Research, Harpenden, Hertfordshire, AL5 2JQ, UK.

Smith, K.L., Colls, J.J. and Steven, M.D., (2005). A facility to investigate effects of elevated soil gas concentration on vegetation. Water Air and Soil Pollution. vol. 161, nº 1-4, 75-96. DOI: 10.1007/s11270-005-2833-x.

Spokas, K., Bogner, J., Chanton, J.P., Morcet, M., Aran, C., Graff, C., Moreau-Le Golvan, Y. and Hebe, I., (2006). Methane mass balance at three landfill sites: What is the efficiency of capture by gas collection systems?. Waste Management. vol. 26, nº 5, 516-525. DOI: 10.1016/j.wasman.2005.07.021.

Tchobanoglous, G., Theisen, H. and Vigil, S.A., (1993). Integrated Solid Waste Management: Engineering Principles and Management Issues. McGraw-Hill.

USEPA, September (1995). User's guide for the industrial source complex (ISC3) dispersión models volumen II – description of model algorithms. U.S. Environmental Protection Agency, Office of Air Quality Planning and Standards Emissions, Monitoring, and Analysis Division Research Triangle Park, North Carolina 27711, EPA-454/B-95-003b.

USEPA, U.S., Environmental Protection Agency, (2005). Landfill gas emissions model (LandGEM) Version 3.02 User's Guide, EPA-600/R-05/047. Office of research and development, National Risk Management Research Laboratory, Air Pollution Prevention and Control Division: Morrisville, NC.

Raufer, R.K. and Wagner, C.P. (1999). Atmospheric Dispersion Modeling. In: Altwicker, E.R.; Canter, L.W.; et. al. Air Pollution. In: David, H.F. Liu and Bela, G. Liptak. eds. Environmental Engineer's Handbook. Boca Raton: CRC Press LLC. DOI: 10.1201/NOE0849321573.ch5.

Vadillo, I. and Carrasco, F., (2005). Estimación del volumen de lixiviado generado en el vertedero de residuos sólidos urbanos de La Mina mediante balance hídrico. Geogaceta. vol. 37, 139 – 142.

Walter, G.R., (2002). Fatal flaws in measuring landfill gas generation rates by empirical well testing. Hydro Geo Chem, Inc. Arizona, USA. http://www.hgcinc.com/fatalflaws.pdf:

Wanichpongpan, W. and Gheewala, S.H., (2007). Life cycle assessment as a decision support tool for landfill gas-to energy projects. Journal of Cleaner Production. vol. 15, nº 18, 1819-1826. dx.doi.org/10.1016/j.jclepro.2006.06.008.

Yalçin, F. and Demirer, G.N. (2002). Performance evaluation of landfills with the HELP (hydrologic evaluation of landfill performance) model: Izmit case study. Environmental Geology. vol. 42, 793–799.

Yen-Cho Chena, Kang-Shin Chenb, Chung-Hsing Wu. (2003). Numerical simulation of gas flow around a passive vent in a sanitary landfill. Journal of Hazardous Materials. vol. 100, nº 1-3, 39–52. dx.doi.org/10.1016/S0304-3894(03)00089-X.

Young, A. and Davies, D., (1992). Application of computer modelling to landfill processes, CWM 039A/92. Mathematical Institute, Oxford University: UK.